Molecular Crystals and Liquid Crystals Science and Technology. Section A. Molecular Crystals and Liquid Crystals

Publication details, including instructions for authors and subscription information:
http://www.tandfonline.com/loi/gmcl19

Transitions in a Spread Film of a Side-Chain Liquid Crystal Polymer

Chris Bower [a], Sarah Froggatt [a], Richard Laycock [a], Rupert J Musgrove [a], Robert M Richardson [a], Greg Rozario [a], Ali Zarbakhsh [a], John P R Webster [b], Oxii Oqx [c], Jonathan S Hill [c], David Lacey [c] & Garry Nestor [c]

[a] School of Chemistry, University of Bristol, Cantock's Close, Bristol, BS8 1TS, U.K.

[b] Neutron Science Division, Rutherford Appleton Laboratory, Didcot, Oxon

[c] School of Chemistry, University of Hull, HU6 7RX, U. K.

Version of record first published: 23 Sep 2006.

To cite this article: Chris Bower , Sarah Froggatt , Richard Laycock , Rupert J Musgrove , Robert M Richardson , Greg Rozario , Ali Zarbakhsh , John P R Webster , Oxii Oqx , Jonathan S Hill , David Lacey & Garry Nestor (1995): Transitions in a Spread Film of a Side-Chain Liquid Crystal Polymer, Molecular Crystals and Liquid Crystals Science and Technology. Section A. Molecular Crystals and Liquid Crystals, 261:1, 437-451

To link to this article: http://dx.doi.org/10.1080/10587259508033488

Mol. Cryst. Liq. Cryst. 1995, Vol. 261, pp. 437–451
Reprints available directly from the publisher
Photocopying permitted by license only

TRANSITIONS IN A SPREAD FILM OF A SIDE-CHAIN LIQUID CRYSTAL POLYMER

CHRIS BOWER, SARAH FROGGATT, RICHARD LAYCOCK,
RUPERT J MUSGROVE, ROBERT M RICHARDSON*, GREG ROZARIO,
ALI ZARBAKHSH
School of Chemistry, University of Bristol, Cantock's Close, Bristol, BS8 1TS, U.K.
JOHN P R WEBSTER
Neutron Science Division, Rutherford Appleton Laboratory, Didcot, Oxon, OX11 OQX, U.K.
JONATHAN S HILL, DAVID LACEY, GARRY NESTOR
School of Chemistry, University of Hull, HU6 7RX, U. K.

Abstract
A series of side-chain liquid crystal polymers have been screened for successful deposition using the Langmuir Blodgett method. It was found that the best materials had glass transitions below room temperature. The behaviour of the spread film of one material was studied in detail using surface isotherms, surface potential, X-ray and neutron reflection techniques. It was found to undergo a phase transition from a thin, low density film to a thicker, more dense one as the surface pressure was increased. This corresponds to a reorientation of the mesogenic units so that about half of them point upwards. At higher pressure a transition to a multilayer occurs on the water surface. In the surface pressure range where deposition is possible, neutron reflection shows that the spread film has a stratum of close packed mesogenic units outermost and the total thickness (38 Å) agrees very well with the smectic layer spacing in the bulk. This similarity in structure could explain the ease of deposition.

* Author for Correspondence

INTRODUCTION

The Langmuir Blodgett (LB) technique provides a method of depositing well ordered multilayers of suitable molecules. However LB films made from low molecular mass materials often suffer from lack of mechanical stability. Polymeric systems offer the possibility of better stability and the method has already been applied to some polymethacrylates[1]. In this paper the possibility of using the technique to process side-chain liquid crystal polymers is explored for a series of siloxane based materials. A number of materials have been screened to see if deposition is practical and a few with good deposition properties have been identified. The nature of spread phases of one of these side-chain liquid crystals on water has been investigated using surface pressure (π) vs. surface area (A) isotherms, surface potential and neutron reflection measurements. The nature of the deposited multilayer films has been studied using X-ray reflection and glancing angle diffraction.

SIDE-CHAIN LIQUID CRYSTAL POLYMER MATERIALS

We have screened a range of polymers, all with mesogenic side-chain units attached to siloxane backbones, based on the structures shown in figure 1. Their preparation and some of their properties are described in references 2, 3, and 4. The different materials are listed in table 1. They all showed smectic or nematic mesophases in bulk samples. All but two of them were prepared from poly-hydrogen-methyl-siloxane (PHMS) . Polymer 2 is a random copolymer of two different mesogenic units joined to the PHMS backbone.

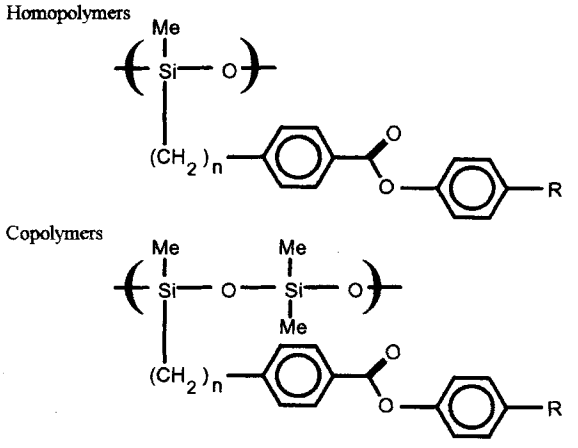

FIGURE 1 Showing molecular structure of side-chain liquid crystal polymers.

Polymers 10 and 11 are prepared from the copolymer poly-hydrogen-methyl-dimethyl-siloxane (PHMDMS) and so have a mesogenic unit attached to every other silicon atom in the chain as shown in figure 1. We tried Langmuir Blodgett deposition of these materials onto silicon substrates using a standard Joyce-Loebl trough with a pure water subphase. The polymers were spread from chloroform solution and deposition was attempted at surface pressures up to about 30 mN m^{-1} where the spread layer collapsed rapidly. Only polymers 1, 3(a racemic version of 1), 10 and 11 gave reasonable deposition of a film. They were found to deposit onto hydrophobic silicon at a pressure of 20 to 30 mN m^{-1}. Of the others, polymers number 2,4,5,6, and 8 did not produce monolayers that were stable enough for deposition while 7, 9 and 12 gave stable spread films but these appeared to be too rigid for successful deposition at room temperature. It was also found that the polymers 10 and 11 are the only ones studied which give reproducible surface pressure-surface area (π-A) isotherms which are discussed in the next section.

TABLE 1 Showing side-chain liquid crystal polymers investigated

Polymer	n	R	backbone	Tg/°C	phase
1	6	$-COOCH_2CH(CH_3)CH_2CH_3$	PHMS	-9	S_C^*
2	6 / 4	-CN / $-C_5H_{11}$	PHMS	—	S_A
3	6	$-COOCH_2CH(CH_3)CH_2CH_3$	PHMS	-25	S_C
4	11	$-C_5H_{11}$	PHMS	80(T_m)	S_A
5	3	$-OCH_3$	PHMS	21	N
6	3	-CN	PHMS	32	S_A
7	3	$-OC_6H_{13}$	PHMS	15	S_A
8	4	-CN	PHMS	26	S_A
9	5	-CN	PHMS	84(T_m)	S_A
10	5	-CN	PHMDMS	-9	S_A
11	6	-CN	PHMDMS	-10	S_A
12	6	-CN	PHMS	18	S_A

Although the variations of the molecular structure are not systematic, it would appear that a low glass transition temperature, Tg, is an important factor in promoting successful LB deposition. Deposition is also unsuccessful below the melting transition temperature, T_m. This is probably because the polymer molecule needs flexibility for successful deposition. The PHMDMS derivatives have low glass transition temperatures and so are good for LB deposition.

Surface pressure-surface area isotherms

Most of the materials did not give reproducible surface pressure-surface area isotherms when spread on pure water: after compression and re-expansion of the through barriers the spread film would remain in a collapsed or partially-collapsed state. We will therefore concentrate our discussion on the isotherm for polymer 11 and a typical (room temperature) isotherm is shown in figure 2 below.

As the area per mesogenic unit is decreased from its initial value of about 50 $Å^2$ the pressure becomes measurable with our equipment at about 40 $Å^2$. There is then a long transition where the pressure only increases gradually. At 17 $Å^2$ the pressure begins to rise steeply. The area per mesogenic unit (i.e. 15 to 17 $Å^2$) in this incompressible region is significantly smaller than the cross section of a single mesogenic unit (about 30 $Å^2$) which suggests that a bilayer may be present. This bilayer would have half of the mesogenic units pointing into the water and half out so that two units could occupy the 30 $Å^2$ on the surface. It seems possible that this transition is a conversion from a monolayer to a bilayer as shown schematically in figure 3. At areas below 15 $Å^2$ per mesogenic unit, a second transition takes place. All these changes are reversible although on re-expansion above 17 $Å^2$ the pressure would generally drop a few mN m^{-1} below the compression values until areas of about 30 $Å^2$ were reached. Since deposition was most successful at pressures above the first transition, we wished to determine the nature of the spread film in this region and the changes that take place during the two transitions.

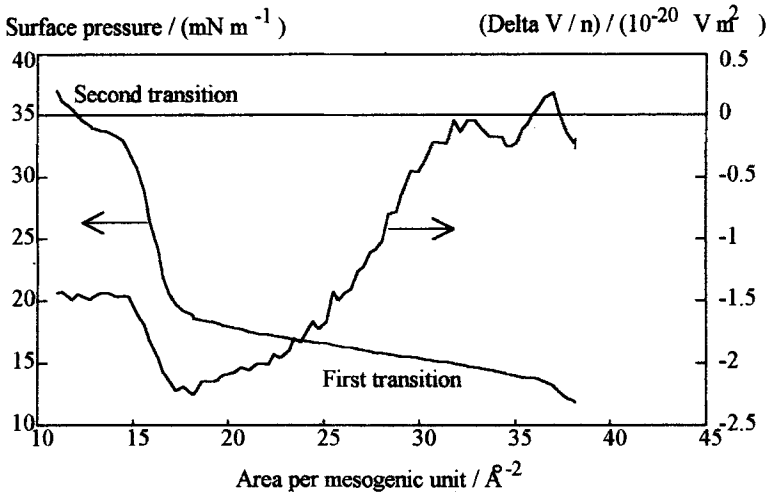

FIGURE 2 Surface pressure and surface potential of polymer 11 as a function of area per mesogenic unit

SURFACE POTENTIAL MEASUREMENTS

The surface potential was measured using an americium 241 (α source) electrode held above the surface during a slow compression of the spread film. The subphase was aqueous 0.01M sodium chloride solution and the second electrode was a simple platinum wire. The potential for a clean surface varied from run to run so the high area per molecule value has been subtracted from each set of potentials to give ΔV. This has been divided by the number of molecules per unit area, n, for each reading during the compression. If the surface potential is determined by a single dipole moment (μ) which makes an angle, θ, with the surface normal, then $\Delta V/n$ will be given by the formula:

$$\frac{\Delta V}{n} = \frac{\mu \cos\theta}{\varepsilon_0 \varepsilon_r}$$

where ε_0 and ε_r are respectively the permittivity of free space and the relative permittivity of the medium around the dipole. Any changes in $\Delta V/n$ may result from changes in the angle or the relative permittivity. The 0.2 V m^2 drop in $\Delta V/n$ (shown in figure 2) on compressing the film from 35 to 17$Å^2$ is consistent with 50% of the CN dipole moments (assuming 4.2 D each) either reorienting by about 180° so that the N atom becomes uppermost or reorienting by a smaller angle with a change in ε_r as the dipole becomes less solvated. Both these possibilities support the monolayer to bilayer transition scheme depicted schematically in figure 3 but they can only be regarded as rather indirect evidence in its favour.

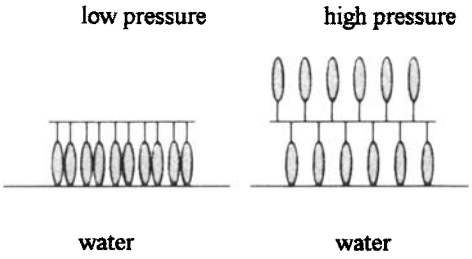

FIGURE 3 Schematic mechanism of transition

X-RAY REFLECTION RESULTS

X-ray reflection[5,6] from the surface of the spread films of polymer 11 on water was used to determine whether the film had collapsed into a multilayer. It was found that at surface pressures below the second transition the reflectivity was qualitatively similar to that of a clean water surface. The small differences from the reflection from a clean interface indicated that the polymer had indeed formed a spread monolayer of similar electron density to water on the surface. However, it was not possible to derive a unique structure for the surface layer by analysing the X-ray reflectivity. At pressures of about 28 mN m^{-1} a pseudo-Bragg peak developed at Q = 0.13 and 0.37 $Å^{-1}$ as shown in

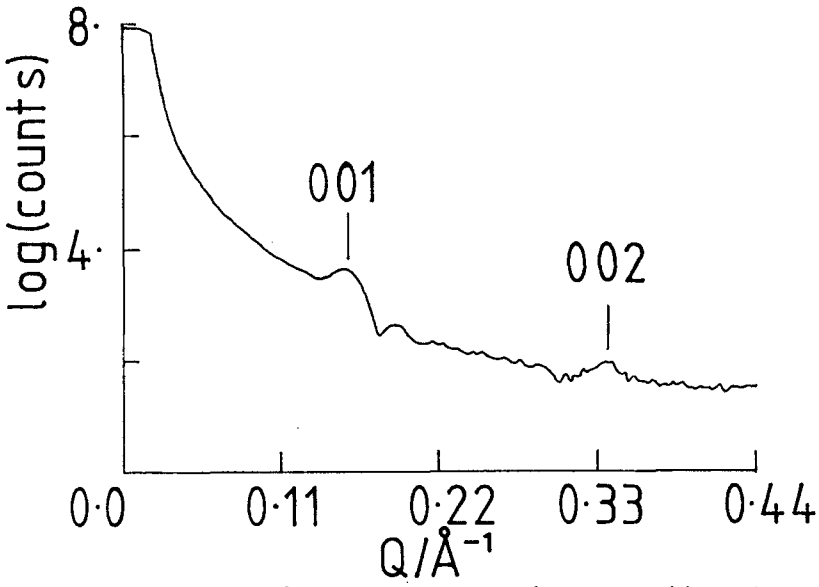

FIGURE 4 X-ray reflection from polymer 11 spread on water with π = 28 mN m^{-1}

figure 4. This indicates that a multilayer with repeat distance of 38 Å is being formed on the surface and suggests that the second transition is a conversion into multilayers. Deposited films also showed this repeat distance and surface diffraction revealed that the layers were very well aligned parallel to the surface. Annealing such samples produced no change in the layer spacing which indicates that the deposited film is in its thermodynamically stable phase (S_A). In some other siloxane based materials[7], it has been found that there are changes on annealing the deposited film. In the next section we report the structure of the spread film at lower pressures which has been determined using neutron reflection.

NEUTRON REFLECTION INVESTIGATION

Theoretical Background

When a beam of neutrons is reflected from the surface of a liquid, a plot of the reflectivity vs. the scattering vector contains information on the surface structure of the liquid. The theory for this has been discussed in detail elsewhere[8,9] but the reflection process is analogous to the reflection of light from a thin film where interference effects are observed. There are two important differences:

i) The wavelength of neutrons is much smaller than visible light so they are very well suited to probing layers that are 10Å to 1000Å thick.

ii) The refractive index for neutrons depends on the scattering length density (SLD), ρ, of the material:

$$\rho = \sum_i N_i b_i$$

where N_i is the number density of the atom type i and b_i is its neutron scattering length. A very useful feature is that it is possible to change the scattering length density (SLD) by varying the isotopic composition of a material, for instance by substituting deuterium ($b = 6.671 \times 10^{-15}$m) for hydrogen ($b = -3.739 \times 10^{-15}$m). Differences in scattering length density are referred to as "contrast" and tend to reflect the incident neutron beam.

In this work we have chosen three different scattering length densities for the aqueous subphase. Air contrast matched (acm) water (i. e. with $\rho = 0.0$ Å^{-2}) has been used because the subphase is then invisible and so interpretation of the results is simple. However it is not possible to determine the position of the polymer with respect to the surface because there is no reflection from the air / acm-water interface. Two other subphase contrasts were used to determine the relative position of the water surface and to obtain more detail about the distribution of the polymer itself. The mean scattering length density of pure polymer 11 has been estimated to be approximately 0.15×10^{-5}Å^{-2} and so reflectivity measurements were made with the scattering length density of the subphase adjusted to have this value by mixing H_2O and D_2O. A layer of polymer with no pronounced internal structure and perhaps mixed with the subphase, would then leave the reflectivity the same as for a clean surface. The final subphase to be used was pure D_2O ($\rho = 0.635 \times 10^{-5}$ Å^{-2}) where the polymer would show up as a layer of lower scattering length density. Figure 5 illustrates the scattering length density profiles that could be anticipated with the three different choices of subphase contrast.

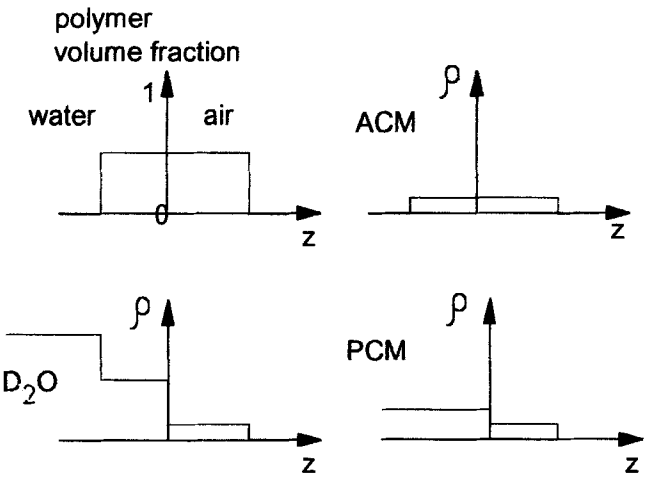

FIGURE 5 Schematic diagram of scattering length density for the same polymer layer with different subphases. z is the distance perpendicular to the surface

It has been found convenient to inspect the data as plots of RQ^4 vs. Q. If a single uniform polymer layer, of thickness d, is present on the surface of the water, the reflectivity (according to the kinematic approximation which holds in the Q-range above the critical edge where the reflectivity is less than ~0.01) is given by the formula:

$$R(Q) \approx \frac{16\pi^2}{Q^4}\left(\Delta\rho_1^2 + \Delta\rho_2^2 + 2\Delta\rho_1\Delta\rho_2\cos(Qd)\right)$$

where $\Delta\rho_1=\rho_F-\rho_A$ and $\Delta\rho_2=\rho_S-\rho_F$ and ρ_A, ρ_F and $\rho_A$are the scattering length densities of the air, film and subphase respectively. For an acm-subphase the kinematic approximation is exact and the relationship becomes:

$$R(Q) = \frac{32\pi^2}{Q^4}\rho_F^2(1-\cos(Qd))$$

It can be seen that a plot of RQ^4 vs. Q will have a sinusoidal form with period $2\pi/d$ from which the thickness, d, can be estimated if both the contrasts (i. e. the $\Delta\rho$'s) are non-zero. The phase of the sine wave will depend on whether $\Delta\rho_1$ and $\Delta\rho_2$ .have the same or opposite signs. These RQ^4 vs. Q plots were very useful methods for making an initial interpretation of the neutron reflection data but the final analysis was done using a full optical matrix calculation[10] of the reflectivity The structure was defined as one or more strata each having a scattering length density ,a thickness and possibly some diffuseness

of the interface with the next stratum. The best values of these parameters were determined by fitting the calculated reflectivity to the measured data. For the acm-subphase it is simple to use this fitting method to determine ρ_F and d for a single stratum model and relate them to the area per mesogenic unit , A , using the formula :

$$A = \frac{\rho_F d}{\sum_i b_i}$$

where the total scattering length of a mesogenic unit (Σb) is 9.25 x 10^{-15} m for polymer 11.

Neutron Reflection Experiments

The neutron reflection experiments were done using the CRISP reflectometer[11] at the Rutherford Appleton Laboratory, Oxon. This reflectometer has a "white" beam and a fixed angle of incidence of 1.5° was used. The absolute scaling of the reflected intensity was determined by measuring the intensity from a pure D_2O / air interface. The data were corrected and reduced to reflectivity vs. scattering vector, Q, using standard programs.

The instrument was fitted with a NIMA computer-controlled Langmuir trough for this experiment. The aqueous subphase was kept at 20°C during the experiment. Surface pressure vs. surface area isotherms were recorded on the spread films before the neutron refection measurements. The isotherm was very similar to that shown in figure 2 except that the first transition plateau extended from about 18 to 52 mN m^{-1}. This results from a slightly different temperature. Neutron reflection measurements were made at pressures of 4 and 8 mN m^{-1} which are at areas above the plateau region, at pressures of 14 and 19 mN m^{-1} which correspond to either end of the plateau and at 26 mN m^{-1} which is approaching the second transition.

Neutron Reflection Results

Figure 6 shows the neutron reflectivity of a spread film of polymer 11 on an air-contrast-matched subphase. These data have been analysed by fitting a single layer model with the scattering length density, ρ_F, and thickness, d, as variable parameters. The interfacial diffuseness was modelled by an error function profile whose standard deviation was held fixed at 3 Å which is a typical value for an air-water interface but which has little effect on the reflectivity at $Q < 0.15$ $Å^{-1}$.. This simple model gave a satisfactory fit to the data for surface pressures up to 14 mN m^{-1} but at higher pressures

some deviations were apparent suggesting that the layer is no longer uniform across its thickness.

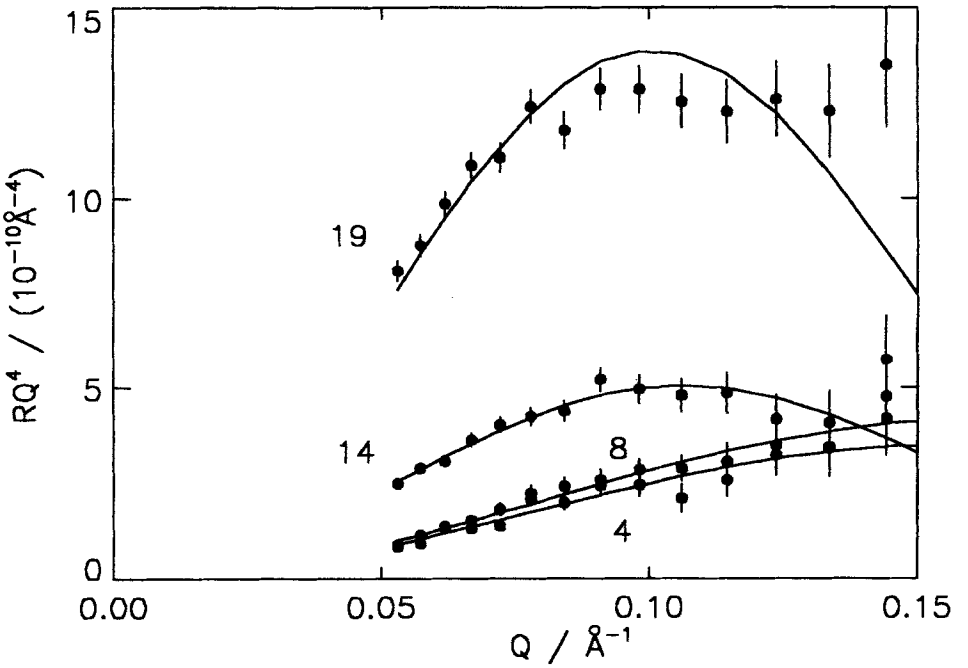

FIGUR E 6 Showing reflectivity from the air-contrast-matched subphase with a spread film of polymer 11. The numbers indicate the surface pressure in mN m^{-1}. The lines are the fits of the single layer model.

TABLE 2. Results from single layer fits to data from air-contrast-matched subphase

π / (mN m^{-1})	d / Å	ρ_F / (10^{-5} Å^2)	Area(R) / Å^2	Area(π-A) / Å^2
4	18	0.084	62	61
8	17	0.093	59	55
14	28	0.094	35	37
19 *	30	0.150	20	19
26 *	35	0.140	19	17

* Single layer model is not a satisfactory fit.

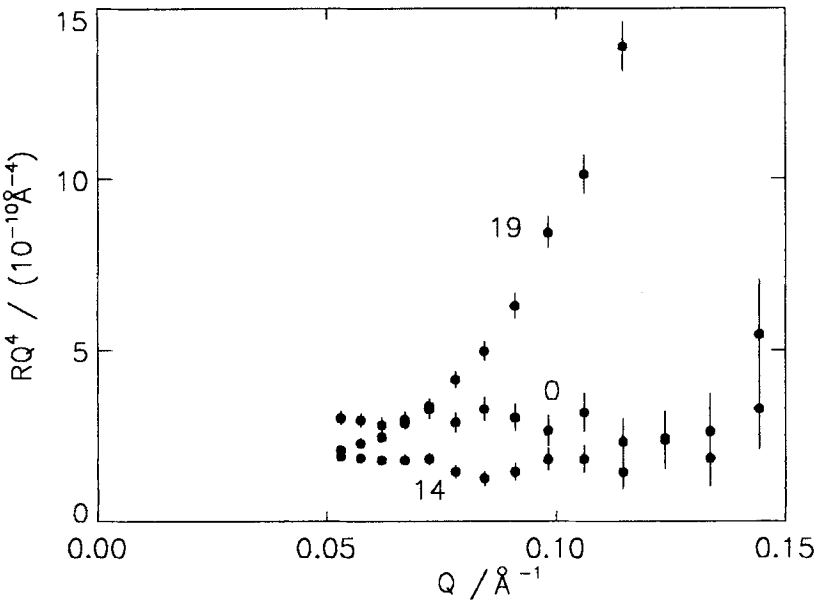

FIGURE 7 showing reflectivity from polymer-contrast-matched subphase with spread film of polymer 11. The numbers indicate the surface pressure in mN m^{-1} with 0 representing the clean surface.

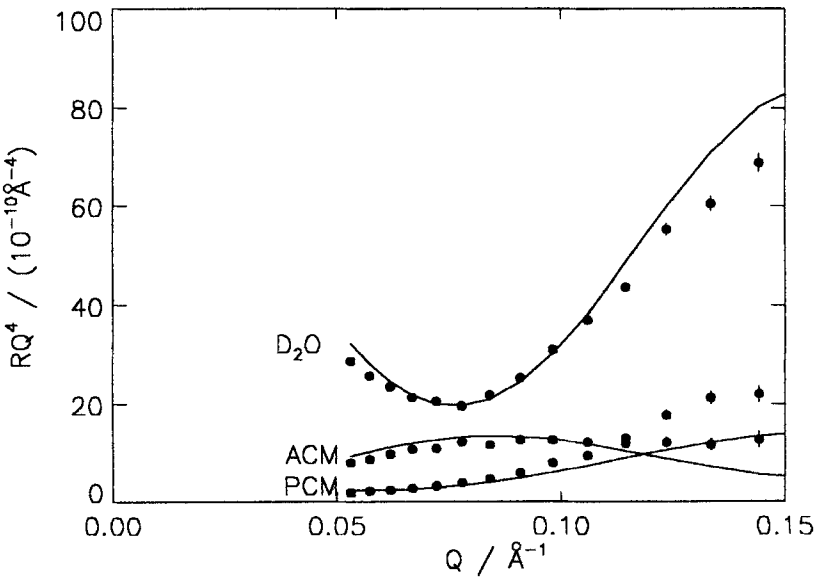

FIGURE 8 showing simultaneous fit to spread film of polymer 11 at 19 mN m^{-1} on three different subphases with spread film of polymer 11. The numbers indicate the surface pressure in mN m^{-1} with 0 representing the clean surface.

The layer thicknesses shown in table 2 are accurate to about 10% whilst the area per mesogenic unit is accurate to 5%. These results show that as the transition is crossed from the high area side, the layer thickness increases from about 17Å to about 30Å. The areas per molecule derived from the reflectivity are also in good agreement with those expected from the pressure - area isotherm that was recorded during the experiment. It is also interesting to note that the scattering length density increases dramatically at pressures above the transition which suggests a denser, more ordered packing of the mesogenic units.

Discussion of Neutron Reflection Results

It seems clear from the results presented above that at a surface pressure of 14 mN m^{-1} and below the polymer film is 17 to 28 Å thick and has a rather open structure indicated by the low scattering length density. At a pressure of 26 mN m^{-1} there is a possibility that multilayer formation was starting. We have therefore concentrated on analysing the 19 mN m^{-1} results to determine the structure of the polymer film above the transition in more detail.

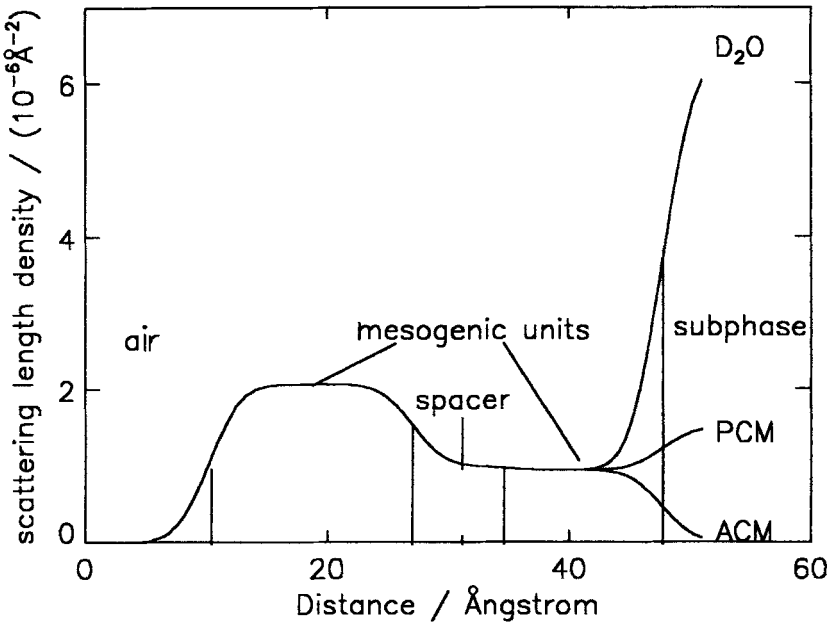

FIGURE 9 showing scattering length density profile corresponding to fits in figure 8

We have found that all three data sets, with different subphase scattering length densities, can be fitted by a three-strata model of the polymer layer. The scattering length density and thickness of each stratum was allowed to vary and the interfacial diffuseness was modelled by a 3 Å error function profile. It was possible to fit data from all three

subphases with this model and the result is shown in figure 8. The fits are not perfect at high Q which may indicate some detail of the model is not quite correct or that the polymer film was not in exactly the same state for the different subphases.

The corresponding scattering length density profiles are shown in figure 9. The scattering length density of the outer layer was found to be 0.2 x 10^{-5} Å^{-2} which is in fair agreement with that expected from close packed mesogenic units (0.25 x 10^{-5} Å^{-2}). The next layer has a lower SLD (0.1 x 10^{-5} Å^{-2}) which is expected if it contains a substantial fraction of siloxane backbone and hydrocarbon spacers which have a SLD of 0.0 x 10^{-5} Å^{-2}. The inner layer is more surprising. Its SLD might be expected to be the same as the outer one but it appears that it is also about 0.1 x 10^{-5} Å^{-2}. This value is similar to that found for the polymer film at lower pressures and suggests that the inner layer is rather open and disordered whereas the outer one is made up of close packed mesogenic units. Any attempt to change the model by incorporating some of the aqueous subphase in the inner layer gave a much worse fit which confirms the expectation that the polymer does not significantly penetrate into the water (i.e. by less than 4 Å). The total distance from the subphase/polymer interface to the polymer/air interface is 38 Å. The fully extended distance from the tip of one mesogenic unit to the tip of another on the opposite side of the backbone as estimated using CPK models is about 48 Å which is about 10 Å more. However the total thickness of the polymer film on the aqueous subphase is in very good agreement with the repeat distance in both a deposited multilayer and the bulk smectic A phase.

The data from the polymer film spread on "polymer-contrast matched" water (i.e. ρ = 0.15 x 10^{-5} Å^{-2}) gives some further insight into the nature of the transition. These reflectivity data are shown in figure 7. It can be seen that at surface pressures up to 14 mN m^{-1} the reflectivity is essentially the same as that of the clean subphase. This suggests that the polymer film is internally disordered so that it has a uniform scattering length density which very similar to that of the subphase. This is expected since ρ_F =0.09 x 10^{-5} Å^{-2} was determined from the analysis of the reflectivity from the acm subphase. Above 14 mN m^{-1} there is a marked deviation from the reflectivity of the clean interface. This also suggests that the polymer forms a film with well ordered strata so that there is a stratum formed by mesogenic units (with a higher scattering length density) separated from the subphase by a stratum containing the polymer backbone and the flexible spacers (with a lower scattering length)

This suggests that the discrepancy between the layer thickness and the model tip-to-tip distance is due to a tilt of the mesogenic units rather than interdigitation with those in the next layer. It also offers an explanation as to why the polymer deposits successfully at surface pressures around 25 mN m^{-1}.At these pressures the spread

polymer layer has approximately the same structure as the bulk material so deposition is a simple laying down of one layer on another without the need to interdigitate the mesogenic units.

CONCLUSION

It has been found that the side-chain polymers with mesogenic units on about half of the silicon atoms have a low T_g, give reproducible behaviour as spread films and can be deposited successfully by the LB method. For polymer 11, we have shown that at surface pressures above the first transition a spread film has a stratum of close packed mesogenic units pointing away from the water. This supports the surface potential evidence that the transition is a rearrangement into a bilayer. The appearance of Bragg reflections means that the second transition is a reversible collapse into a multilayer. It appears that there is little rearrangement of the layers on deposition (from spread films at pressures between the two transitions) since the spread polymer layer has the same total thickness as the repeat distance in the deposited material.

ACKNOWLEDGEMENTS

We gratefully acknowledge the help given by Mr. A Makepeace and Mr. S. Neck of Bristol University in setting up the Langmuir trough.

REFERENCES

1. A. F. Thibodeaux, R. S. Duran, H. Ringsdorf, A. Schuster, A. Skoulios, P. Gramain and W. Ford, Macromolecular Assemblies in Polymeric Systems, edited by P. Stroeve and A. C. Balzazs (ACS Symposium Series no. 493), Chap. 3, pp. 20-30
2. G. Nestor, G. W. Gray, D. Lacey and K. J. Toyne, Liquid Crystals, 6, 137-150 (1989)
3. G. W. Gray, J. S. Hill and D. Lacey, Makromol. Chem., 191, 2227-2235 (1990)
4. R. M. Richardson, G. W. Gray and A. R. Tajbakhsh, Liquid Crystals, 14, 871-879 (1993)
5. R. M. Richardson and S. J. Roser, Liquid Crystals, 2, 797-814 (1987)
6. N. Dent, M. J Grundy, R. M. Richardson, S. J. Roser, N. B. McKeown, and M. J. Cook, J.de Chimie Physique, 85, 1003-1008 (1988).
7. W. Rettig, J. Naciri, R. Shashidhar, R. S. Duran, Thin Solid Films, 210, 114-117 (1992)

8. M. J. Grundy, R. M. Richardson, S. J. Roser, J. Penfold and R. C. Ward, Thin Solid Films, 159, 43-52 (1988).
9. J. Penfold and R K Thomas, J. Phys. Condens. Matter, 2, 1369 (1990)
10. F. Abeles, Ann.de Physique, 3, 504 (1948)
11. J. Penfold, R. C. Ward and W G Williams, J. Phys. E, 20, 1411 (1987)